Research Summary

The Direct Metal Deposition of H13 Tool Steel for 3-D Components

J. Mazumder, J. Choi, K. Nagarathnam, J. Koch, and D. Hetzner

The rapid prototyping process has reached the stage of rapid manufacturing via the direct metal deposition (DMD) technique. The DMD process is capable of producing three-dimensional components from many of the commercial alloys of choice. H13 tool steel is a difficult alloy for deposition due to residual stress accumulation from martensitic transformation; however, it is the material of choice for the die and tool industry. This article reviews the state of the art of DMD and describes the microstructure and mechanical properties of H13 alloy deposited by DMD.

INTRODUCTION

In manufacturing, the limiting time for many products is the design and fabrication of molds and dies of all types. It is not unusual for large complicated dies to take weeks or months to almost a year before they are ready to manufacture a product. Stereolithography has been a help in the design process for visualizing a component produced directly from a computer-aided design (CAD) database by curing polymers with lasers. Most manufacturers are looking for a device that can make a product or design directly from a CAD drawing. Repair procedures are also needed for metals that do not change the material properties, resulting in reduced life for the product.

Preliminary work on the direct metal deposition (DMD) of aluminum has demonstrated the provision of metal properties equivalent to a wrought process, thus, making it potentially useful for the direct fabrication of parts and dies.[1] Almost all other processes for developing metal result in a sintered product due to the trapping of oxides and the inability to completely bond. As a result, they attempt to fill the metal matrix and do not provide the strong properties demonstrated by DMD. If there is a total bonding and no oxides or sintered properties, the metal property has generally been significantly affected, as is the case in a welded-type structure that is built up by repeated passes. In these cases, significant heat treatment is needed to make the part useful and to relieve the stresses. Laser-aided DMD limits these problems since it creates a very small heat-affected zone. DMD can be used on almost any surface and can mix metals to create a variety of properties, including graded structure, exhibiting similar potential as droplet-based manufacturing.[2-6] However, DMD has a wider range of deposition capability.

The DMD process should have no environmental concerns since the process is additive and does not create waste products. It is carried out in an inert atmosphere, with powdered metal dropped on the point and melted at that spot. Health and safety concerns only appear to be the result of laser operations, and there are procedures for these conditions available.

A recent survey by the National Center for Manufacturing Science (NCMS) revealed that DMD can reduce the time for die production by 40 percent.[7] Typically, it may take 3–40 weeks for die production using present technology; DMD has the potential to save several billion dollars in the U.S. die production industry, which currently costs $10.8 billion.

The DMD process allows for either the direct production of a part or short-time, low-cost delivery of molds or dies. When perfected, the process will greatly reduce costs

Figure 1. The DMD process.

EXPERIMENTAL PROCEDURES

A chromium-molybdenum hot-work die steel, H13, was directly deposited onto substrates of wrought H13. This alloy, commonly used in die casting, was analyzed because of its potential high-volume usefulness in the rapid manufacturing of die-casting tooling. Heat-treatment comparisons for both DMD and wrought H13 were performed in the areas of "as-clad" hardness, ductility, and microstructure; initial tempering response; and tempering response for austenitized (1,010°C), oil-quenched material.

To replicate a commercial system, two cladding-deposition modes were analyzed. A low-power, low-metal deposition rate was selected since this processing corresponds to the parameters used for details and edges. A high-power, high-metal deposition rate mode of operation was used since this corresponds to the method used for adding bulk material. These two forms of processing are referred to as fine and course cladding, respectively.

The operating conditions used for coarse cladding consisted of a 1.1 mm focus spot rastered to 3.5 mm for the fabrication of a thick, one-dimensional vertical wall. The laser power was 4,500 W and the powder-feed rate was 16 g/min. The powder was delivered perpendicular to the raster direction. The beam and the powder flow were turned off at the end of each pass, and subsequent layers were accumulated while translating 750 mm/min. in the same direction. Successive layers were deposited to create a 3.5 mm wide, 70 mm tall, and 120 mm long build-up onto a low-carbon steel substrate. During this processing, the temperatures of the clad were not measured, but visible radiation was observed after the first 5–10 layers were deposited. A tensile bar oriented perpendicular to the clad direction was machined from this as-clad specimen (Figure A). During tensile testing, an extensometer measured strain in the gage section.

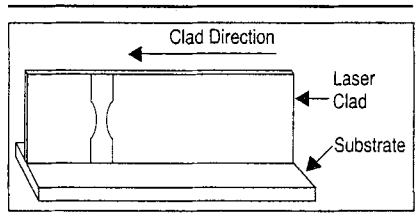

Figure A. The laser-cladded geometry and tensile specimen orientation.

For fine cladding, the metal powder and shroud gas were delivered concentrically. The molten pool was formed by a 0.6 mm diameter spot. The specimen velocity for both types of cladding processes was 750 mm/min. The laser power and powder-feed rate were 1,000 W and 5 g/min. for the fine processing. A feedback system monitored the height of the molten pool as the specimen was traversed in a stitching pattern. The thickness of each deposited layer was 250 μm. The pattern was repeated to create a slab 90 mm high. H13 was used for both the substrate and clad to allow a direct comparison between the laser-clad and wrought material in the ensuing heat-treating experiments.

From the laser-cladded substrates, specimens were cut and then sealed inside quartz tubes under vacuum for heat treating. One group of specimens was tempered for two hours at temperatures ranging from 375°C to 650°C. Another group of specimens was austenitized at 1,010°C, quenched in oil, and then tempered for two hours at temperatures ranging from 400°C to 650°C.

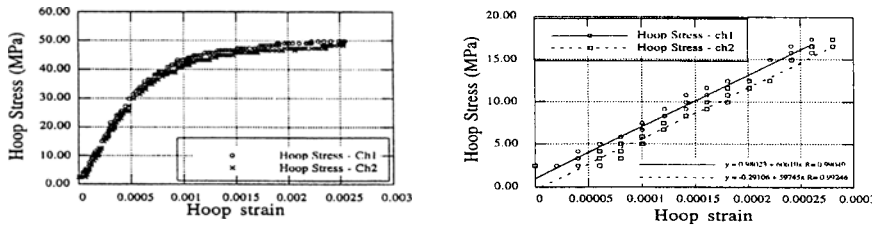

a b

Figure 2. Hoop stress vs. strain curves for (a) a pressurized cylinder and (b) the elastic region.

and time in getting a prototype or product ready for use. This is an example of a situation that would benefit a wide variety of products for both defense and commercial sectors. The ability to make low-volume, high-quality parts directly from CAD is applicable to most of the U.S. Department of Defense (DOD) manufacturers. The U.S. Navy has also expressed interest in this process as it would allow an aircraft carrier to go out with barrels of metal and CAD drawings to make parts as they are needed, eliminating the need to carry a large inventory of spare parts. The automotive and electronics industries can use the application for the rapid fabrication of dies.

Many international groups are actively pursuing DMD for commercial possibilities. The direct fabrication of molds and dies and the repair of these parts is the most

Table I. Rapid Prototyping Techniques

Commercial Process Name	Phenomena	Depth/Layer (mm)	Layers/Hour	Surface Roughness	Total Deposition Rate	Ref.
Stereo Lithography	Point-to-point laser cure	0.10–0.50	Variable	> 5 μm	~4.0 in^3/h	9, 10, 13, 16–17, 19–21
Solid Ground Curing	Masked exposure with ultraviolet	0.10–0.15	60–100	0.1% of part dimension	N/A	15, 20
Selective Laser Sintering	Sintering of powder layers	0.12	80–400	± 0.125–± 0.25	N/A	10, 15, 20
Fused Deposition Modeling	Extruded thermoplastic	0.02–0.12	Variable	± 0.127 mm	N/A	9, 15, 20
Laminated Object Manufacturing	Bonded profile-cut sheets	0.05–0.50	Variable	> 0.127 mm	N/A	9, 10, 15, 20
Hot Pot	Laminated polystyrene sheets	0.5	N/A	N/A	N/A	20
Designed-Controlled Auto Fabrication	Masked exposure with ultraviolet	0.0125 minimum	90	N/A	N/A	15, 20
SOMOS/Soliform	Point-to-point laser cure	0.12–0.50	Variable	> 5 μm	N/A	20
Solid Creation System	Point-to-point laser cure	0.10–0.30	Variable	> 5 μm	N/A	20
Computer-Operated Laser Active Modeling	Point-to-point laser cure	N/A	N/A	± 0.1–± 0.5 mm	N/A	15, 20
Stereos	Point-to-point laser cure	N/A	N/A	0.02 mm	N/A	15, 20
Solid Object Ultraviolet Laser Plot	Point-to-point laser cure	N/A	N/A	± 0.05 mm	N/A	15, 20
Light Sculpting	Masked exposure with ultraviolet	0.0127	N/A	0.00254 mm	N/A	15
Developmental Technique						
Ballistic Particle Manufacturing	Point- by-point droplet deposition	N/A	N/A	6.35 mm	12,000 droplets/sec. with d = 0.003 in droplet	9, 15, 20
Incre	Point-by-point droplet depostion	N/A	N/A	N/A	N/A	20
Electrosetting	Layered electrodes	N/A	N/A	N/A	N/A	20
MD-Star	Sprayed materials on masks	0.025–0.10	N/A	N/A	N/A	20
Photochemical Machining	Dual plane laser cure	N/A	N/A	N/A	N/A	20
Shape Melting	Continuous cast GMA welding	N/A	N/A	N/A	N/A	20
3-D Printing	Select binder to powder	0.076–0.254	N/A	1.3–3.0 mm	N/A	9, 15, 20
Laser Cladding	Point-by-point fused metal	0.10–1.50	Variable	0.1–0.5 mm	0.1–4.0 $cm^3/min.$	1, 12, 14 16, 18
Droplet-Based Manufacturing	Molten metal droplets	N/A	N/A	N/A	0.02–0.25 mm/sec. with d = 0.178 mm droplet	2, 4–6

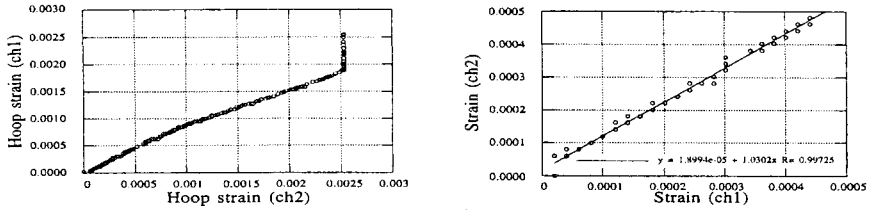

Figure 3. (a) Strain vs. strain for 2,500 microstrains and (b) elastic strain vs. strain.

obvious application. However, the fabrication of low-volume parts has not been fully analyzed and may be the biggest potential for this process. Surgical instruments have been explored, and the potential savings are in the hundreds of millions of dollars. For surgical tools, DMD can reduce 62 steps into seven steps.[7] The use of the process in the aerospace business is another possible area for applications. Probably the most promising future application is the distributed manufacturing of functional components by transferring data through the Internet.

The scientific challenge is to control the dimension and properties of the process. Close control of dimension will result in substantial savings in post-process machining cost for surface finish. Substantial cost reduction is possible, if desired properties can be achieved through process control and minimizing the post-process heat treatment. Control of the meltpool size and solidification time can offer both desired dimension by limiting the meltpool volume and desired properties through microstructure manipulation by controlling the cooling rate. This will require quantitative understanding of the relationship between independent process parameters (e.g., laser power speed, powder deposition rate, etc.), dimension, cooling rate, microstructure, and properties by developing fundamental understanding of the associated transport phenomena. Strategies for on-line process control will also be required to achieve the desired meltpool volume and cooling rate.

DIRECT-METAL DEPOSITION

Rapid prototyping and rapid manufacturing directly from a CAD database has created tremendous contemporary interest; about 24 techniques are under investigation by different groups all over the world. Various techniques that have been published in the open literature are compared and summarized in Table I. Only a very few techniques have the capability of producing metal parts directly from the CAD database with near 100% density and functional properties. Most of the polymer-based techniques are only good for design visualization, whereas, DMD offers the possibility of fabricating a 100% dense-metal component with functional properties.

In DMD, a laser generates a melt pool on a substrate material while a second material is delivered into the meltpool either as powder or as wirefeed that melts and forms a metallurgical bond with the substrate (Figure 1). A turbine disc of circular geometry was produced by Breinan and Kear[8] via layer-by-layer laser cladding around 1978. Presently, computer-controlled, five-axis workstations integrated with lasers enable manufacturers to fabricate various geometries. Initial work carried out at the University of Michigan has demonstrated that components with mechanical properties similar to plate materials can be fabricated, even from oxide formers such as aluminum[1] as well as copper, nickel, and ferrous alloys.

In testing, a volume deposition of 4.1 cm^3/min. was measured for traverse speed of 42.3 mm/sec. About 90 percent of the dispensed powder was utilized for a clad 0.4 mm thick and 4 mm wide. The powder-utilization ratio varied from 30–90 percent, depending on the width of the deposit layer. The higher the width, the better the utilization ratio. The as-deposited surface roughness was found to be similar to that of a cast structure. The best possible resolution for wall thickness using a 6 kW CO_2 laser is around 0.5 mm, whereas, Los Alamos National Laboratory has deposited 0.25 mm wall thickness using a yttrium-aluminum-garnet (YAG) laser. However, the deposition rate will be smaller for higher accuracy. Nevertheless, it was already demonstrated that a wide range of deposition rates and geometrical resolutions may be possible with laser-based DMD as a function of the laser power and beam quality.

Initial data on DMD (based on laser cladding) aluminum indicate that the strength of the final product is comparable to the published strength data for plate materials.[1] Mechanical tests were conducted on the one-dimensional flat plate and a two-dimensional cylinder. For the plate, uniaxial tensile specimens

Figure 4. A micrograph of fine cladding.

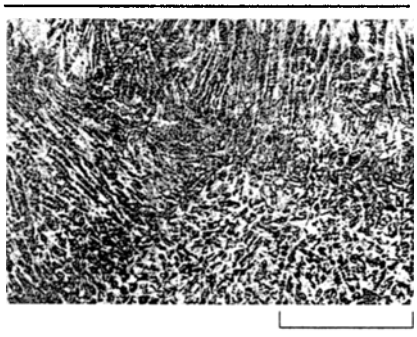

Figure 5. Fine cladding.

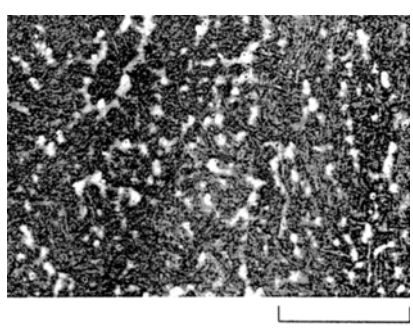

Figure 6. Course cladding.

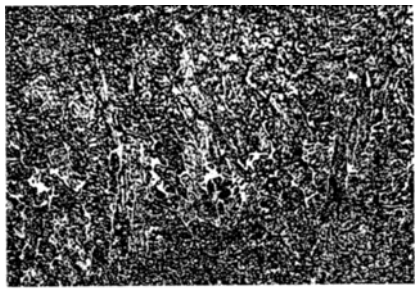

Figure 7. Fine clad tempered at 500°C.

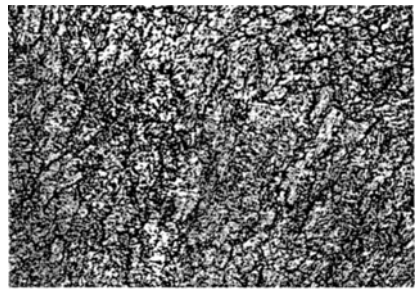

Figure 8. Fine clad tempered at 600°C.

were milled both parallel (axial) and perpendicular (transverse) to the clad direction. Eleven specimens were machined with a gage-section length of 10 mm and a cross-sectional area of 8.9 mm^2. An extensometer was fixed to each specimen to generate stress-strain data for each uniaxial test. The 0.2% yield stress ranged from 35–40 MPa for the axial specimens and 37–42 MPa for the transverse, while the axial specimens had a slightly higher strength out at the final strains. The specimens were not taken to fracture because of their tremendous ductility. Also, distinct, visible slip bands were found exclusively perpendicular to the clad direction.

An aluminum cylinder was also fabricated by the DMD technique and pressure tested. The original wall thickness of 3 mm was machined down to 1 mm. A mandrel was built with two O-rings and a passage for hydraulic oil to exert internal pressure. The two strain gages were mounted perpendicular to the axis, halfway between the two Orines and 180° relative to each other. Both the strain and internal pressure via a 6.7 MPa, full-scale pressure transducer were monitored with data-acquisition equipment throughout the entire test. A hand pump pressurized the vessel to a final strain of 4.3% before a defect ruptured. For the pressurized cylinder, hoop stress (σ_{hoop}) was calculated from internal pressure (P) with

$$\sigma_{hoop} = P\,(r_i/t)$$

where r_i was the internal radius (23.81 mm) and t was the wall thickness (0.98 mm). Figure 2a shows stress-strain plots for both strain gages, while Figure 2b shows the elastic region where a modulus of elasticity of 60,000 MPa was calculated. As a whole component, it was able to sustain well over the 35 MPa yield stress for aluminum.

In order to evaluate the uniformity of deformation, Figure 3a shows strain vs. strain for the two gages. The two strains are nearly equal (slope = 1.03) in the elastic region (Figure 3b) and begin to deviate from each other as the component undergoes plastic deformation. Overall, the component was able to sustain a hoop stress greater than its 35 MPa-rated yield stress.

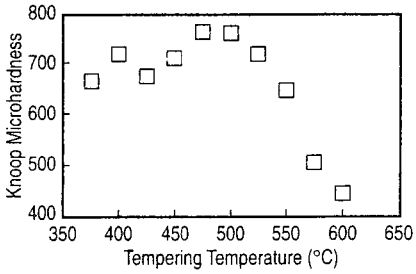

Figure 9. The tempering response of laser-clad H13.

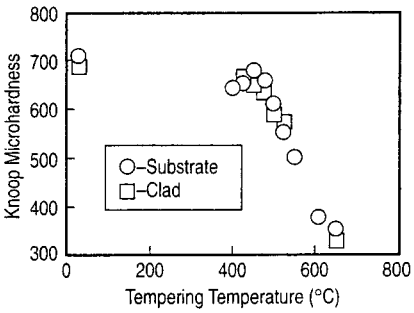

Figure 10. The tempering response for austenitized H13.

MICROSTRUCTURAL RESULTS

The as-clad microstructure of the fine processing consists of four zones (Figure 4). The bulk of the substrate corresponds to the typical structure of fully annealed H13. The matrix is ferrite and contains numerous small bands of alloy carbides. Just below the clad is the heat-affected zone of the substrate. This is the dark etching zone consisting of tempered martensite. The majority of the clad is dark etching, although the last, or top, layers are light etching. As the first clad layer is deposited, it cools very quickly as heat is extracted by the substrate; the microstructure at this stage is untempered martensite. As each additional clad layer is deposited, heat from the solidifying material passes through the previously deposited clads into the substrate. Hence, the preliminary clads become tempered; tempered martensite is dark. Since the uppermost layers of the clad have not been tempered, they are still light etching.

The relationship between dendrite arm spacing and solidification rate has been studied by other investigators. For the clads deposited by the fine processing, the

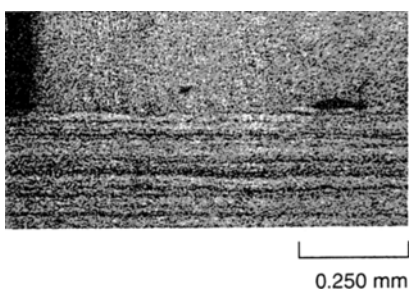

Figure 11. A micrograph of austenitized and tempered H13.

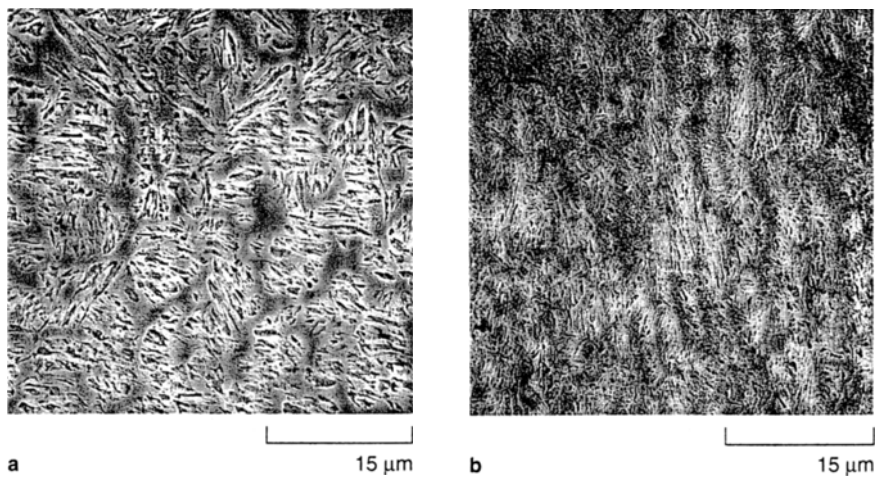

Figure 12. Scanning electron micrographs of the laser-processed H13 coating microstructures where (a) P = 3 kW and v = 152 cm/min. and (b) P = 2 kW and v = 330 cm/min.

Table II. Residual Stress Measurement on a H13 Tool Steel Specimen

Location/Depth	Residual Stress (MPa) Long.	Perp.	45 Deg.	Trans.	Peak Width (deg.)
Loc. 1/0.609 mm	–6.69 ±0.138	—	–3.65 ±0.138	1.24 ±0.138	1.65
Loc. 2/Surface	–10.27 ±2.894	—	–9.03 ±1.379	–3.31 ±1.861	5.33
Loc. 3/0.508 mm	–0.14 ±0.414	—	0.69 ±0.138	0.07 ±0.007	1.92
Loc. 4/0.685 mm	—	+2.90 ±0.345	+5.58 ±0.276	+10.55 ±0.276	1.90
Loc. 5/Surface	—	+ 32.13 ±0.552	—	—	4.51
Loc. 6/Surface	—	+ 34.06 ±0.621	—	—	4.62

center-to-center dendrite cell spacing is approximately 4 μm (Figure 5). Assuming H13 is somewhat similar to maraging steel and austenitic stainless steel, this cell spacing corresponds to a solidification rate on the order of 100°C/sec. Dendrite spacing for course processing is approximately 20–30 μm and is not accurately extrapolated (Figure 6).

The microstructure of the H13 in the as-clad condition is primarily tempered martensite with some retained austenite. The light etching structure between the dendritic cells in the as-clad H13 is alloy carbides. For tempering temperatures up to 500°C, very little change in microstructure is noted (Figure 7). For tempering temperatures of 600°C and higher, the dendritic-carbide network begins to break up into smaller individual carbides. As this transformation occurs, the regions that were previously light etching are now dark etching, and the cell boundaries are more clearly delineated (Figure 8).

For the as-clad condition, secondary hardening occurs when tempering temperatures are between 400°C and 500°C (Figure 9); however, it is not possible to see this effect by optical microscopy. At temperatures above 500°C, the hardness of the deposited clad rapidly drops. This corresponds to the microstructural changes noted in Figure 8.

Tempering occurs in the heat-affected zone at 600°C. The dark etching, non-martensitic transformation product that formed during cladding becomes light etching. This is caused by the reprecipitation of fine alloy carbides and the formation of ferrite.

When austenitized, quenched, and tempered, the behavior of the laser-clad and wrought H13 is very similar (Figure 10). The alloy softens as the tempering temperature increases; however, some secondary hardening occurs between 400°C and 500°C. The wrought alloy seems to have a slightly greater amount of secondary hardening than the clad steel. The microstructures of the clad and wrought H13 in the heat-treated condition are very similar. Both constituents contain tempered martensite and some retained martensite and austenite. After austenitizing at 1,010°C for one hour, most evidence of the dendritic-solidification structure in the clad has been removed by diffusion. However, banding caused by alloy segregation is still evident in the wrought substrate (Figure 11).

Figure 12 shows the laser DMD H13 with a traverse speed of 152 cm/min. and 330 cm/min., respectively. Microstructural refinement with increasing speed can be observed.

MECHANICAL PROPERTIES AND RESIDUAL STRESS

A traverse of microhardness across the fine clad and wrought substrate verifies the martensitic structure (Figure 13). The average hardness was 690 Knoop and 675 Knoop for the fine and course clads, respectively. A tensile bar was machined from the course clad. The monotonic test revealed a yield strength of 1,505 MPa and an ultimate strength of 1,820. The six percent strain at failure and ten percent reduction in area was equal to or better than wrought H13 of equal hardness.

The management of residual stress and resultant distortion is a critical factor for the success of this process in demonstrating the production capability of three-dimensional components. Residual-stress accumulation is the biggest cause of cracking during the fabrication of tool-steel components. In order to get some preliminary understanding of stress generation, a sample is designed to estimate the stress accumulation per layer.[9] This helped to develop a strategy to build up multiple layers before the accumulated residual stress can lead to cracking. After the deposition of a predetermined number of layers, stress relieving is carried out before further layers are deposited. This strategy led to successful fabrication of a fullsize IMS-T1 component (Figure 14).

The fabricated sample was sent to Lambda Research for residual-stress measurement. Figure 14 also shows the points where stress was measured. Locations 2, 5, and 6 are deposited during the last run and, thus, show residual compressive stress, since they were not stress relieved. The other locations were deposited in earlier runs and were subsequently stress relieved. They show negligible residual stress, whereas the maximum stress at the location without stress relieving is +34.06 MPa (Location 6, Table II).

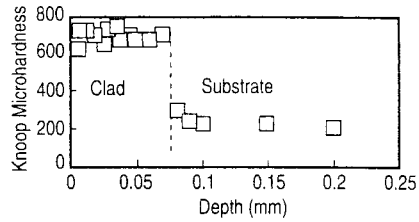

Figure 13. The microhardness traverse of laser-clad annealed substrate.

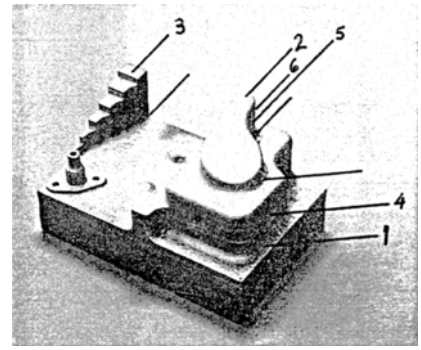

Figure 14. Initial results of residual stress in G13 tool steel. See Table II for measurement values.

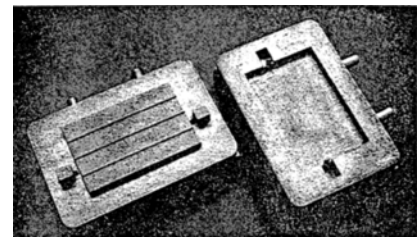

Figure 15. Injection molding dies with imbedded copper chill block and a water-cooling channel.

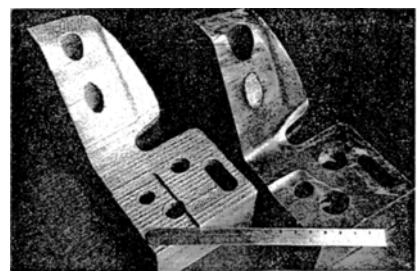

Figure 16. A trimming die.

Recently, different components have been successfully fabricated for various sponsors. Injection molding dies with imbedded copper chill bock (Figure 15) and water-cooling channel was delivered for one sponsor. A trimming die (Figure 16) was fabricated for another. All components had dimensional tolerances within a few thousands of a centimeter.

ACKNOWLEDGEMENT

Most of the work reported in this article was carried out when the authors were at the University of Illinois. Funding from the National Science Foundation, Delphi-Packard, and Magna Corporation made this work possible.

References

1. J.L. Koch and J. Mazumder, *Rapid Prototyping by Laser Cladding*, ed. P. Denney, I. Miyamoto, and B. L. Mordike (Orlando, FL: ICALEO, 1993), pp. 556–565.
2. J.H. Chun and C.H. Passow, "Droplet Based Manufacturing" (Paper presented at the Conference in International Rapid Prototyping, 1993).
3. P.J. Acquaviva, T. Nowak, and J.H. Chun, "Issues in Application of Thermal Spraying to Metal Mold Fabrication" (Paper presented at the International Body of Engineers Conference, 1994).
4. M. Orme, "On the Genesis of Droplet Stream Microspeed Dispersions," *The Physics of Fluids A*, 3 (12) (1991), pp. 2936–2947.
5. M. Orme, "Droplet Patterns from Capillary Stream Breakup," *The Physic of Fluids A*, 5 (1) (1993), pp. 80–90.
6. M. Orme, "Rapid Solidification Materials Synthesis with Nano-Liter Droplet, Education, Training, and Human Engineering in Aerospace," *Aerotech '93*, (Costa Mesa, CA: SAE, 1993).
7. J. Westmoreland, National Center for Manufacturing Science, private communication.
8. E.M. Breinan and B.H. Kear, "Rapid Solidification Laser Processing of Materials for Control of Microstructure and Properties," *Proceedings of Conference on Rapid Solidification Processing at Reston, VA*. (Baton Rouge, LA: Claitor's Publishing Division, 1978), p. 87.
9. S. Ashley, "Rapid Prototyping is Coming of Age," *Mechanical Engineering*, 117 (7) (1995), pp. 62–68.
10. D.A. Beleforte, "Rapid Prototyping Speeds Product Development," *Laser Focus World*, 29 (6) (1993), pp. 126–133.
11. J.H. Chun and C.H. Passow, "Droplet Based Manufacturing," (Paper presented at the Conference in International Rapid Prototyping, 1993).
12. J. Gerken, H. Haferkamp, and H. Schmidt, "Rapid Prototyping/Manufacturing of Metal Components by Laser Cladding," *Conference on Rapid Prototyping for the Automotive Industries and Laser Applications for the Transportation Industries, Vol. 7* (Aachen, Germany: Automotive Automation Limited, 1994), pp. 85–91.
13. P.F. Jacobs, *Fundamentals of StereoLithography* (Dearborn, MI: Society of Manufacturing Engineers, 1992), p. 434.
14. Y.J. Jeng, in Ref. 12, pp. 273–279.
15. D. Kochan, "Solid Freeform Manufacturing—Advanced Rapid Prototyping," (Elsevier, Amsterdam: 1993), p. 211.
16. W. Konig, I. Celi, and S. Noken, in Ref. 12, pp. 253–263.
17. W. Konig, Y.-A. Song, and T. Celiker, in Ref. 12, pp. 281–288.
18. E.W. Kreutz et al., "Rapid Prototyping with CO_2 Laser Radiation," *Applied Surface Science*, 86 (1995), pp. 310–316.
19. H. Narahara, "Accuracy Improvement Procedures for Stereolithography Parts," *International Journal of the Japan Society for Precision Engineering*, 28 (4) (1994), pp. 301–304.
20. J.M. Pachenco, *Rapid Prototyping—MTIAC SOAR-93-01* (Chicago, IL: Manufacturing Technology Information Analysis Center, 1993).
21. R.W. Pfeiffer, "Stereolithography Accuracy: Influence of Photosensitive Materials," (Paper presented at the Third International Conference on Rapid Prototyping, Dayton, OH, 1992).

ABOUT THE AUTHORS

J. Mazumder earned his Ph.D. at Imperial College, London University. He is a professor at the University of Michigan.

J. Choi earned his Ph.D. in mechanical engineering at the University of Illinois at Urbana–Champaign in 1994. He is currently a research fellow at the University of Michigan.

K. Nagarathnam earned his Ph.D. in mechanical engineering at the University of Illinois at Urbana–Champaign in 1994. He is currently a research fellow at the University of Michigan. Dr. Nagarathnam is a member of TMS.

Justin Koch earned his M.S. in mechanical engineering at the University of Illinois at Urbana–Champaign in 1985. He is currently a project engineer for Caterpillar.

Daniel Hetzner earned his Ph.D. in metallurgical engineering at the University of Tennessee in 1980. He is currently a research specialist.

For more information, contact J. Mazumder, University of Michigan, 2250 G.G. Brown Building, Ann Arbor, Michigan 48109-2125; (313) 647-6824; fax (313) 763-5772; e-mail mazumder@engin.umich.edu.